COMPDYN 2015
5th ECCOMAS Thematic Conference on
Computational Methods in Structural Dynamics and Earthquake Engineering
M. Papadrakakis, V. Papadopoulos, V. Plevris (eds.)
Crete Island, Greece, 25–27 May 2015

RAILWAY-INDUCED GROUND VIBRATIONS IN THE PRESENCE OF LOCAL TRACK IRREGULARITIES AND WHEEL FLATS

G. Kouroussis[1], G. Alexandrou[1], D. P. Connolly[2], K. Vogiatzis[3], and O. Verlinden[1]

[1]University of Mons — UMONS, Faculty of Engineering,
Place du Parc 20, B-7000 Mons, Belgium
e-mail: {georges.kouroussis,georgios.alexandrou,olivier.verlinden}@umons.ac.be

[2] Heriot-Watt University, School of Energy, Geoscience, Infrastructure & Society,
Edinburgh EH14 4AS, United Kingdom
e-mail: d.connolly@hw.ac.uk

[3] University of Thessaly, School of the Civil Engineering,
Pedion Areos, 383 34 Volos, Greece
e-mail: kvogiatz@uth.gr

Keywords: wheel/rail impact, vehicle/track interaction, ground-borne vibration, environmental impact assessment, flat wheel, local track irregularities

Abstract.

Rapid growth in railway infrastructure has led to numerous environmental technical challenges. This includes ground-borne vibration, which is becoming an increasing problem, particularly in urban environments. A common source of this vibration is local defects (e.g. rail joints, switches and crossings) which cause large amplitude excitations at isolated locations. Modelling this type of excitation mechanism using typical linear frequency domain analysis is challenging and therefore non-linear time domain methods are required. Therefore, in this study a validated and comprehensive time domain, three-dimensional ground vibration prediction model is used to investigate the vibrations generated at the wheel/rail contact due to local rail and wheel surface defects. Different types of rail and wheel defect are mathematically modelled, including rail joints, switches, crossings and wheel flats. The track is modelled as a typical ballasted track, using a two-step approach where the vehicle/track dynamics and ground wave propagation are simulated separately. The first step models the effect of railway vehicles (using a multibody approach with many degrees of freedom) on the dynamic excitation of the track and incorporates a non-linear Hertzian contact law at the wheel/rail interface. The second step applies these track-vehicle model forces to a finite/infinite element model to accurately generate vibration time histories for required ground-borne vibration assessment. This work focuses on the AM96 trainset, largely used in the Brussels Region (Belgium). The geometries of a variety of local defect types are analysed and a sensitivity analysis is undertaken based on the defect size and train speed. It is found that defect type and geometry have a significant influence on vibration levels, and that only selected geometry types are effected by train speed.

1 INTRODUCTION

Much research into railway-induced ground vibrations has focused on the effect of high-speed trains on the environment. This is motivated by the so-called "supercritical phenomenon" which appears when the vehicle speed is close to the Rayleigh ground wave speed. The latter depends on the soil flexibility and may be close to that of conventional high-speed lines [1, 2]. Despite the large vibration levels generated by these lines which are underlain by soft soils [3], the distance d between the track and neighbouring structures is relatively high and the vibration attenuates rapidly. In the case of railway traffic, the attenuation is associated with a power law of the form d^{-q}, where q lies between 0.5 and 1.1, depending on the soil configuration [4]. Connolly et al. [5] proved that it is possible to establish relationships between six key railway variables for ground vibration metrics in the case of high-speed lines. The situation is significantly different in the case of urban transit, due to the presence of local defects which induces elevated localised vibrations (dynamic effect).

The latter observation represents the main contribution of dynamic excitation in railway track. The pioneering work of Nielsen and Abrahamsson [6], Zhai et al. [7] and Oscarsson, Andersson and Dahlberg [8, 9] focus on the interaction between the track and the vehicle, in order to establish accurate models. They take into account the different elements of the track/foundation system. Similar work was recently done by Kouroussis et al. [10] to prove that an accurate simulation of track/soil interaction is important in the prediction of ground-borne vibration [11]. These numerical approaches offer the possibility of studying local defect effects on track dynamics. The study of vehicle/track coupling with local defects and the associated degree of dynamic coupling are of growing interest. The influence of vehicle-flexible mode shapes on the ride quality has been investigated [12], including local geometrical imperfections. Zhao et al. [13] employ a three-dimensional finite element model to evaluate the wheel/rail impact forces at local rail surface defects. They also evaluate the resulting dynamic forces at the discrete supports of the rail under different rolling speeds.

The aforementioned studies focus on the track/vehicle whereas few studies have analysed the effect of local defects on ground vibration. Despite this, many ground-borne vibration complaints in urban environments are due to local rail and wheel surface defects (e.g. switches, rail joints, ...). Kouroussis et al. [14] quantify the vibration generated by a tram running on a local rail defect using a numerical model in two successive steps (vehicle/track). Using the same approach, Alexandrou et al. [15] also study the wheel flat effect on ground motion and analyse the influence of wheel flat size. Vogiatzis [16, 17] undertakes a large-scale analysis of ground vibrations generated by underground Athens metro lines by studying wheel flat impact forces as impulses. As the source of vibration results from the wheel/rail contact, it is essential to study vehicle interaction with the track and the soil. Therefore, Costa et al. [18] show the importance of integrating a multibody model of the vehicle in the track/soil simulation and that in the case of a distributed rail's unevenness, sprung masses have minimal effects on the ground vibration motion. Furthermore, Kouroussis et al. [19] conclude that the choice between a simple model or a detailed model for the vehicle depends upon the importance of wheel and rail unevenness.

The purpose of this paper is to show the effect of typical rail and wheel surface defects. The study utilizes a numerical two-step approach, previously validated for this kind of situation. It focuses on the AM96 trainset circulating in Brussels, for which substantial measured data exists [20]. The present work deals with a layered soil based on geophysical tests performed at the same test site. In order to compile a dataset of the main parameters that influence ground vibration levels, different defect geometries are considered for various train speeds and defect

sizes.

2 CLASSIFICATION OF LOCAL DEFECTS

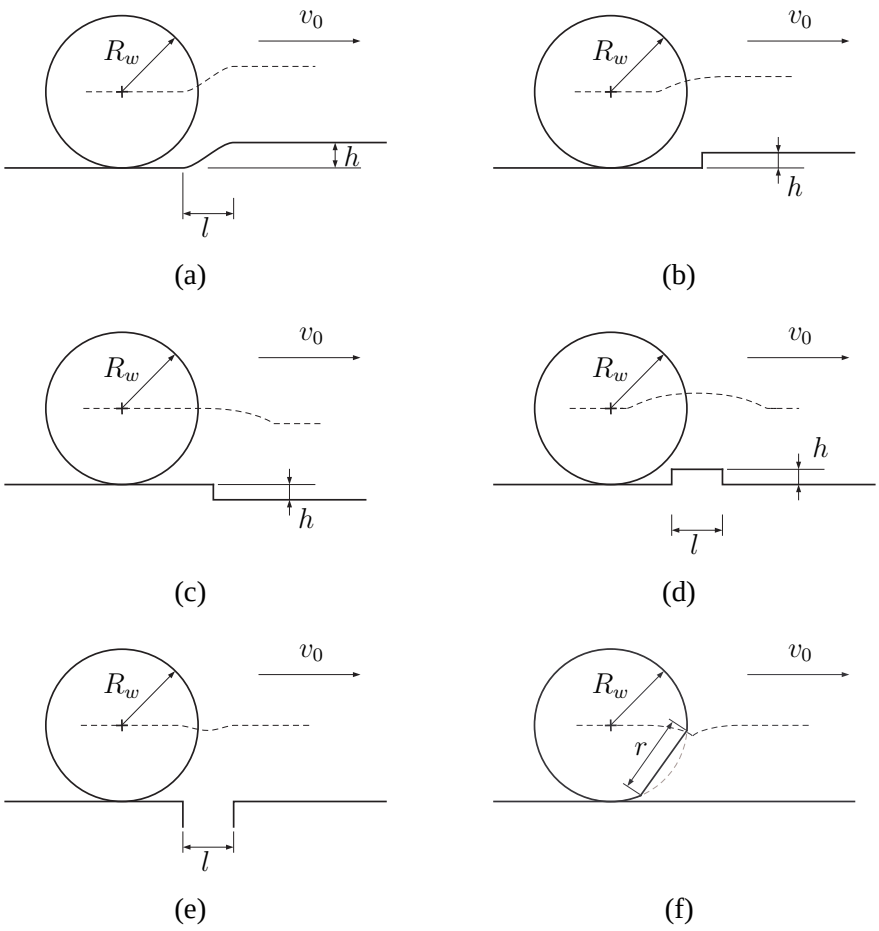

Figure 1: Mathematical modelling of local rail and wheel surface defects: (a) smooth irregularity, (b) step-up joint, (c) step-down joint, (d) stepwise joint (step-up), (e) stepwise joint (step-down) and (f) wheel flat.

Figure 1 presents the mathematical interpretation deduced from defects encoutered in practice. It shows the local discontinuity encountered in urban areas that commonly contribute to ground vibration generation. For each defect, the dimensions are presented (illustrated by the solid line under the wheel in Figure 1), and the shape "seen" by the wheel/rail interface (illustrated by the dotted line in Figure 1) which can be different than the defect shape, taking into account the wheel radius R_w and the vehicle speed v_0.

3 NUMERICAL MODEL

The proposed prediction model is based on two successive calculations [21]. Complexity required the problem to be split. This approach allows the most well-suited modelling approach to be used for each subsystem. First of all, the dynamics of the vehicle/track subsystem is simulated by considering a multibody vehicle model moving at speed v_0 on a flexible track with a rail irregularity (Figure 2). The wheel/rail forces are defined using non-linear Hertz's theory and allows coupling between the vehicle model and the track. The latter is defined as a flexible beam (Young modulus E_r, geometrical moment of inertia I_r, section A_r and density ρ_r) discretely

supported by the sleepers (of mass m and with spacing d), including viscoelastic elements for the ballast (stiffness k_b and damping coefficient d_b) and the railpads (stiffness k_p and damping coefficient d_p). To take into account the dynamic behaviour of the foundation, which plays an important role at low frequencies, a coupled lumped mass (CLM) model is added to the track model, with interconnection elements for the foundation-to-foundation coupling [22]. A C++ object-oriented program was developed, using the in-house EasyDyn library [23]. An application based on a symbolic engine platform generates mathematical kinematic expressions for the vehicle. The generalized coordinates approach is used to obtain a system of pure ordinary differential equations, without constraint equations. The symbolic engine platform creates a C++ code directly compilable against the EasyDyn library. The problem definition is completed by generating applied forces (suspensions, wheel/rail contact) and a link to the track model (which is already established and depends on site parameters only). An implicit scheme is used for the simulation in this first step. The ballast reactions are then saved and used as input forces for the second step.

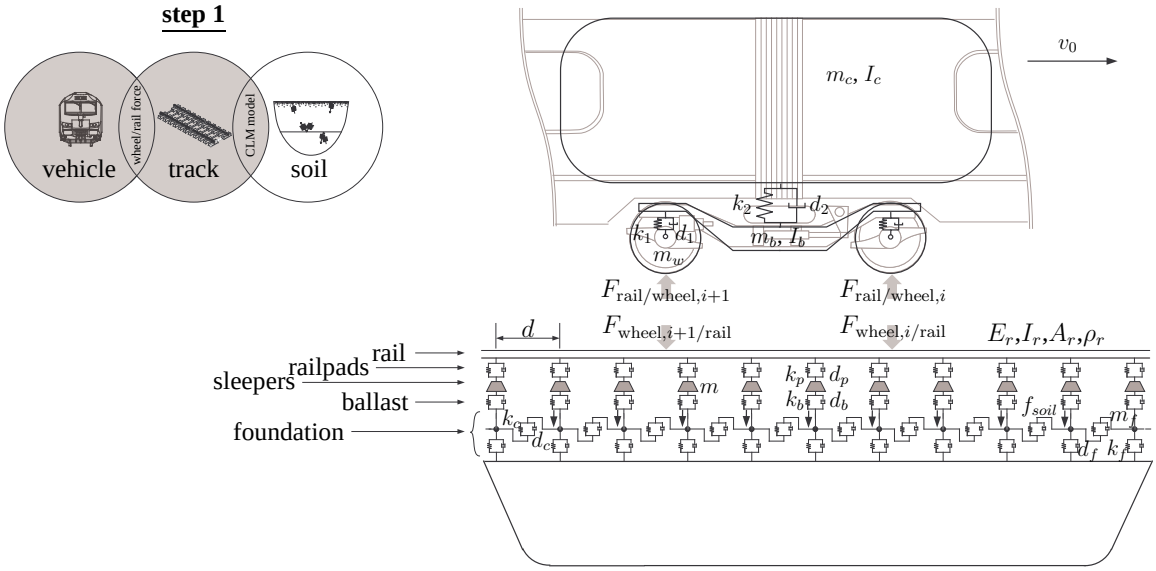

Figure 2: Description of the prediction model: vehicle/track/foundation simulation.

The second step addresses the dynamics of the soil subsystem, with the soil surface forces representing the contribution from the sleepers (Figure 3). The dynamic ground response is calculated using the finite element method, which is well suited for 3D analysis. Some analyses were recently conducted by the authors to improve the performance of their finite element model [24], namely:

- *Complex geometry*. A fully 3D finite element model allows treating complex geometry (track embankment, inclined layer interfaces). Moreover, variability in track profile and high ground vibrations originating in singular rail surface defects can be treated without any difficulty.

- *Non-reflecting boundary conditions*. The combined use of viscous boundaries and infinite elements provides more efficient non-reflecting condition than classical setups (free or fixed boundaries). Here, the small dependence on incident wave angle and dynamic parameters is quantitatively carried out for each solution. A spherical soil border geom-

etry is defined, to which infinite elements are attached. This convex shape configuration insures the condition of non-crossing infinite elements.

- *Reasonable computation time*.The simulation in time domain is an interesting solution to study ground vibrations in a relatively small region of interest. As ground vibrations are inherently a transient phenomenon, the time domain analysis is appropriate to simulate wave propagation and does not impose any condition on the domain size, which would be required in the frequency domain. Moreover, the equations of motion describing the soil dynamics are integrated using explicit central difference integration to reduce the computational burden.

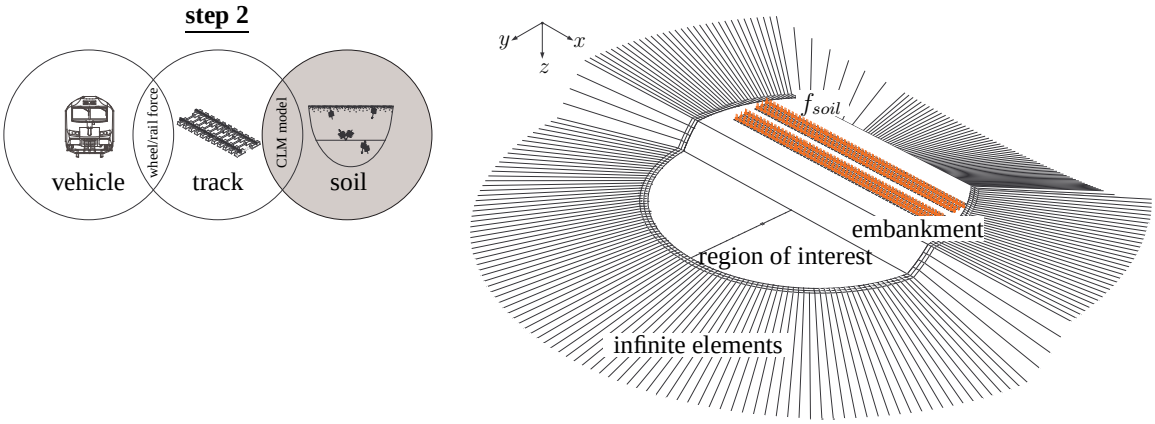

Figure 3: Finite element soil modelling using infinite elements and viscous boundary conditions.

4 NUMERICAL SIMULATIONS AND RESULTS

This study focuses on the InterCity train operating in Brussels (Belgium). The AM96 trainset, largely used by the Belgian Railway Operator, SNCB, is typically used for InterCity and InterRegion connections. This study evaluates the AM96 trainset's generation of elevated ground vibration levels in comparison to other domestic trains [20]. It consists of three carriages, designated HVBX, HVB, and HVADX. The HVBX leading wagon is equipped with motorised bogies, whereas the HVB (middle) and HVADX (end) wagons are trailer carriages. Figure 4 represents the configurations and the positions of each wheelset on the vehicle. A classical multibody approach is used and limits the vehicle dynamics to pitch and bounce motions.

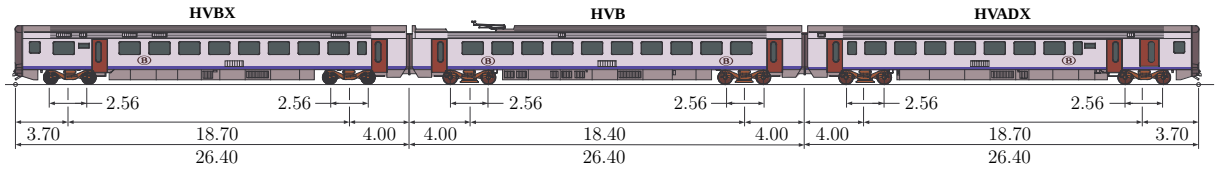

Figure 4: Configuration of the AM96 electric multiple unit.

4.1 Free-field ground vibrations

Figure 5 presents an analysis of the numerical results, considering the cases without defect and with a step-up stepwise joint representing a pulse defect (vertical height $h = 5\,\mathrm{mm}$ and horizontal length $l = 10\,\mathrm{mm}$). The AM96 trainset runs at a speed v_0 of $120\,\mathrm{km/h}$. The comparison

is based on the time history of numerical velocities in the vertical direction (Figure 5(a)) and the corresponding normalized frequency content (Figure 5(b)), both for a distance of $10\,\mathrm{m}$ from the track. A significant difference in levels is observed between the two cases' velocity traces (more than ten times magnification). The passing of each wheelset is more clearly defined in the case where the defect is present. Although the frequency content is spread over a range $[0;100\,\mathrm{Hz}]$, all dominant frequencies are located in the frequency range 0 – $60\,\mathrm{Hz}$.

The frequency spectra present some similarities. For instance, both datasets identify several dominant frequencies due to the fundamental and harmonic carriage frequencies. Moreover, the fundamental axle and bogie passage frequencies imply a double amplitude modulation, as considered in [19]. The effect of distance from the track is also analysed. As presented in Figure 5(c), it shows the far field peak particle velocity, PPV, defined as the maximum absolute amplitude of soil surface velocity in the vertical direction. The investigations are based on a track with an embankment: receivers are placed out the embankment area (in the far field) where ground vibration is most likely problematic.

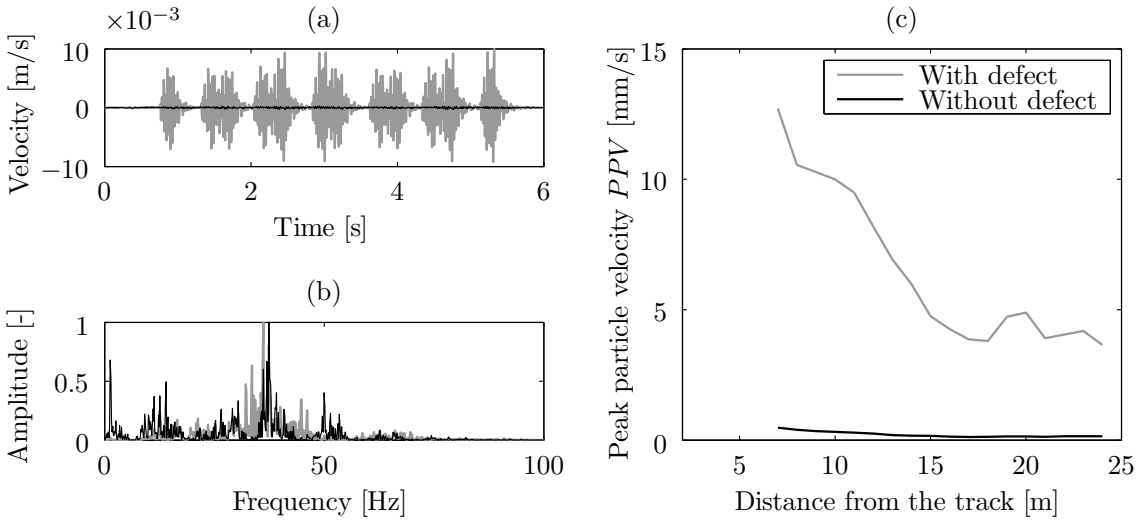

Figure 5: Comparison between numerical data (grey: with $5\,\mathrm{mm}$ height pulse defect; black: without defect) related to the passage of an AM96 trainset (2×3 carriages) at a speed v_0 of $120\,\mathrm{km/h}$, (a) time histories at $10\,\mathrm{m}$ from the track, (b) frequency contents at $10\,\mathrm{m}$ from the track and (c) Peak particle velocity as a function of the distance from the track.

Figure 6 demonstrates the associated ground wave propagation for the same aforementioned defect. It gives a comprehensive view of the free field response on the soil's surface. The selected time histories emphasize the instants when the first bogie crosses the local defect. At times before $t = 0.75\,\mathrm{s}$, the ground wave generation is due to the quasi-static contribution of the vehicle (no contact with the local defect). At times after $t = 0.75\,\mathrm{s}$, the ground wave propagation is amplified by the wheel/defect contact due to the vehicle/track dynamics. This effect is visible until $t = 1\,\mathrm{s}$, showing that the phenomenon is transient and affects each wheel/defect impact.

4.2 Influence of the defect type

The six shapes of discontinuity presented in Figure 1 (representing various defect types such as transition zones, switches, crossings, rail joints, and wheel flats) are analysed in this section. The case of an AM96 trainset running at a constant speed v_0 and separately interacting with

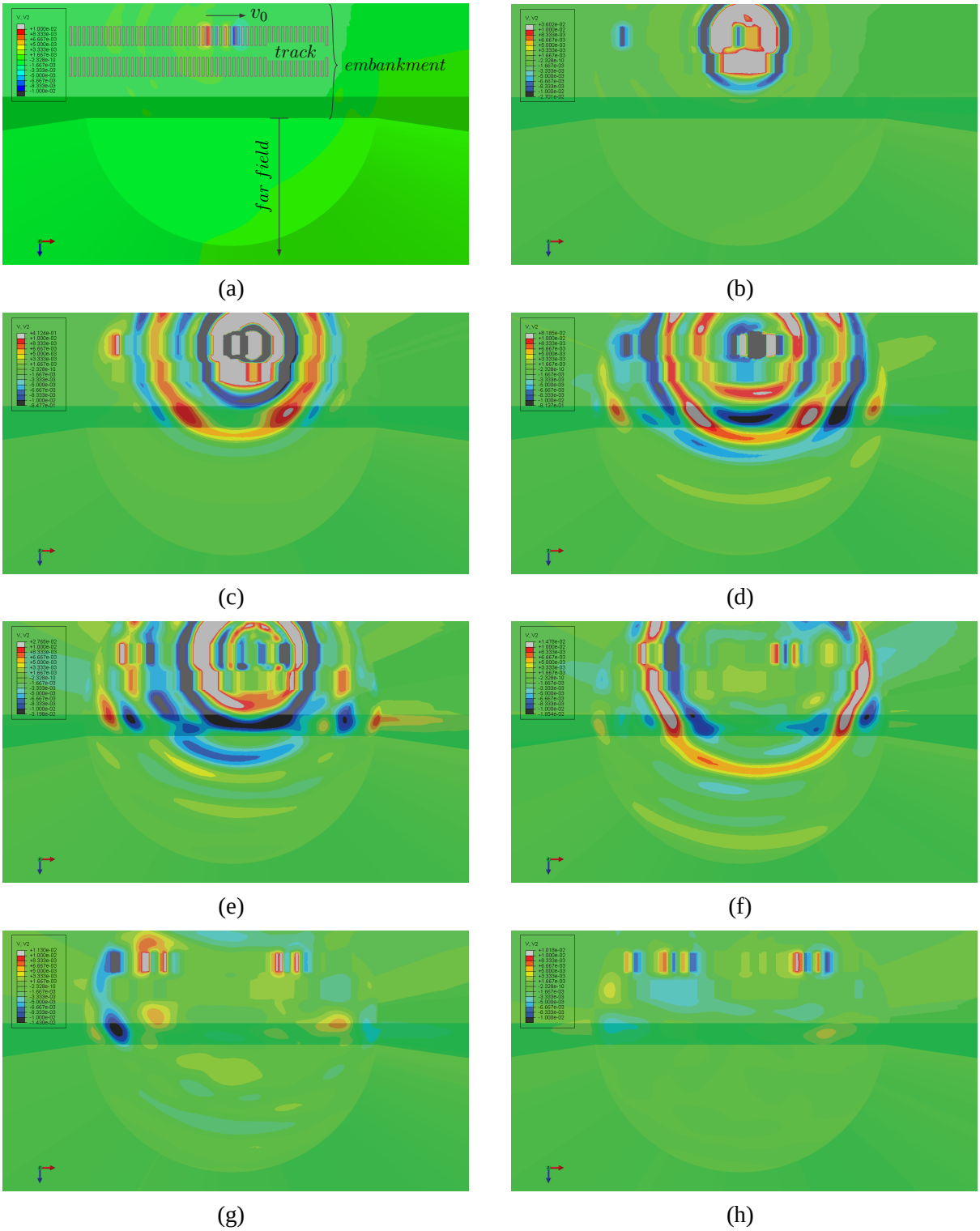

Figure 6: Birdseye view visualisation of the passage of an AM96 trainset at a speed of $120\,\mathrm{km/h}$ on a $5\,\mathrm{mm}$ height pulse defect: free field vertical component of the soil vibration waves (a) at $0.7\,\mathrm{s}$, (a) at $0.75\,\mathrm{s}$, (b) at $0.8\,\mathrm{s}$, (c) at $0.85\,\mathrm{s}$, (d) at $0.9\,\mathrm{s}$, (e) at $0.95\,\mathrm{s}$, (f) at $1.0\,\mathrm{s}$, (g) at $1.05\,\mathrm{s}$.

these defects is studied.

Figure 7 presents the level of surface ground vibration at different distances from the track, in a region outside the embankment. The values of defect length and size were selected according

to those commonly found in practice. For the smooth irregularity (ramp function), the length l is $200\,\mathrm{mm}$ (sufficiently long to replicate a smooth transition zone) with a height $h = 10\,\mathrm{mm}$. For the pulse function (step-up stepwise joint), the length is fixed at $l = 10\,\mathrm{mm}$ with a height $h = 5\,\mathrm{mm}$. For the negative pulse function (step-down stepwise joint), the length is fixed at $l = 20\,\mathrm{mm}$. For the other rail defects, only the height is relevant, and is fixed as $h = 5\,\mathrm{mm}$. The flat spot is selected with a length $r = 30\,\mathrm{mm}$. The results show large discrepancies between ground vibration levels, with very small levels for the step-down stepwise joint and wheel flat, which were close to those obtained without local defects (Figure 5(c)). Specifically, a difference in results between the step-up and step-down joint cases occurs as a result of symmetrically identical geometry. This is due to the non-linear effects at the wheel/rail contact where climbing and dropping do not represent the same dynamic effect. The change in vibration level with the distance from track offset has a general tendency to decrease.

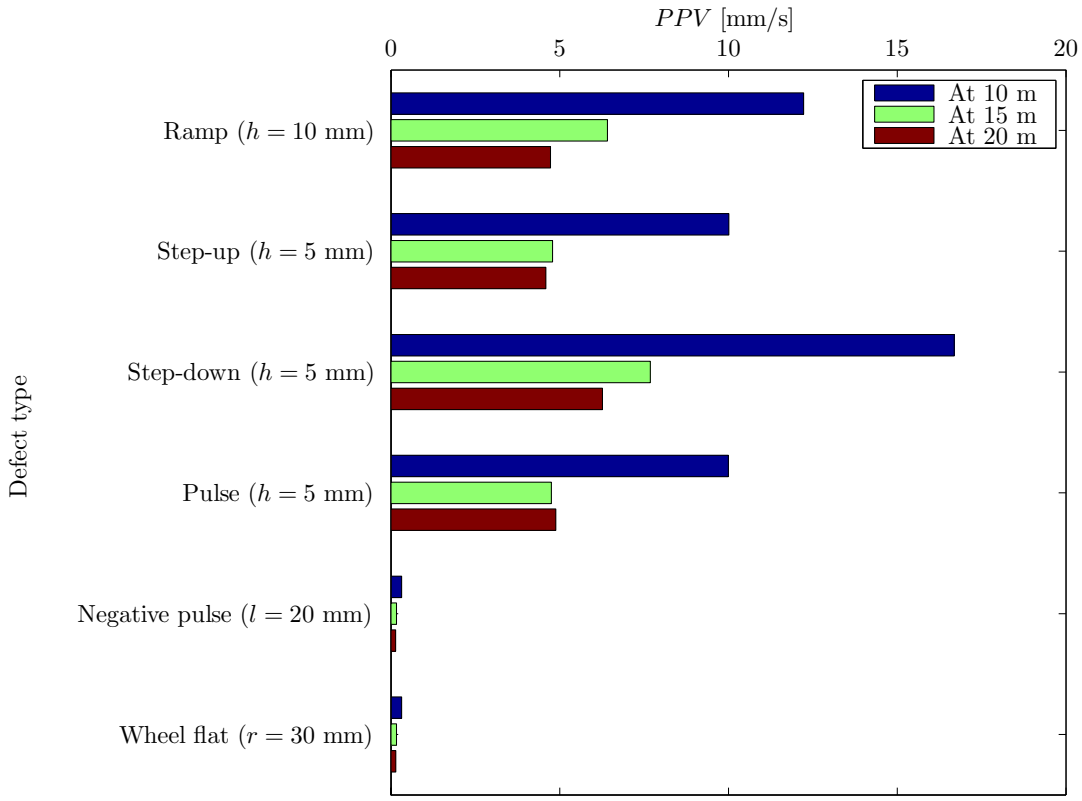

Figure 7: Peak particle velocity as a function of the distance from the source and the defect type for an AM96 trainset running at $120\,\mathrm{km/h}$.

4.3 Influence of the defect size

A sensitivity analysis is presented in Table 1 for when the main dimension varies (h for the smooth irregularity, the step-up joint, the step-down joint, step-up stepwise joint; l for the step-down stepwise joint; r for the wheel flat). Generally, there is a positive relationship between the PPV and defect size.

At $120\,\mathrm{km/h}$, the wheel flat and negative pulse have zero effect on ground vibrations. This is due to the vehicle speed shifting the frequency content to a higher range. These high frequencies are are then rapidly dampened by the soil and the track, meaning that at the studied distances,

	$l = 200\,\mathrm{mm}$	$l = 200\,\mathrm{mm}$	$l = 200\,\mathrm{mm}$
	$h = 5\,\mathrm{mm}$	$h = 10\,\mathrm{mm}$	$h = 15\,\mathrm{mm}$
Smooth irregularity	$4.78\,\mathrm{mm/s}$ $(-61\,\%)$	$12.23\,\mathrm{mm/s}$	$20.64\,\mathrm{mm/s}$ $(+69\,\%)$
	$h = 2.5\,\mathrm{mm}$	$h = 5\,\mathrm{mm}$	$h = 7.5\,\mathrm{mm}$
Step-up joint	$4.29\,\mathrm{mm/s}$ $(-57\,\%)$	$10.01\,\mathrm{mm/s}$	$11.43\,\mathrm{mm/s}$ $(+14\,\%)$
	$h = 2.5\,\mathrm{mm}$	$h = 5\,\mathrm{mm}$	$h = 7.5\,\mathrm{mm}$
Step-down joint	$2.13\,\mathrm{mm/s}$ $(-87\,\%)$	$16.69\,\mathrm{mm/s}$	$28.49\,\mathrm{mm/s}$ $(+71\,\%)$
	$l = 10\,\mathrm{mm}$	$l = 10\,\mathrm{mm}$	$l = 10\,\mathrm{mm}$
	$h = 2.5\,\mathrm{mm}$	$h = 5\,\mathrm{mm}$	$h = 7.5\,\mathrm{mm}$
Step-up stepwise joint	$4.06\,\mathrm{mm/s}$ $(-59\,\%)$	$10.00\,\mathrm{mm/s}$	$10.31\,\mathrm{mm/s}$ $(+3\,\%)$
	$l = 10\,\mathrm{mm}$	$l = 20\,\mathrm{mm}$	$l = 30\,\mathrm{mm}$
Step-down stepwise joint	$0.32\,\mathrm{mm/s}$ $(-0.4\,\%)$	$0.32\,\mathrm{mm/s}$	$0.32\,\mathrm{mm/s}$ $(+1\,\%)$
	$r = 20\,\mathrm{mm}$	$r = 30\,\mathrm{mm}$	$r = 40\,\mathrm{mm}$
Wheel flat	$0.32\,\mathrm{mm/s}$ $(+0.5\,\%)$	$0.32\,\mathrm{mm/s}$	$0.32\,\mathrm{mm/s}$ $(+0.5\,\%)$

Table 1: Ground vibration level at $10\,\mathrm{m}$ from the source for an AM96 trainset running at $120\,\mathrm{km/h}$.

their effect is insignificant. Figure 8 illustrates this by comparing the ground wave propagation generated by the train's passing. In Figure 8(a), the reference case without a defect is presented and Figure 8(b) is related to the case with a defect. The same colour scale is used in both results (vertical acceleration is displayed in order to more clearly emphasize the high frequency content), showing the difference between the two cases observed in the near-field's embankment area.

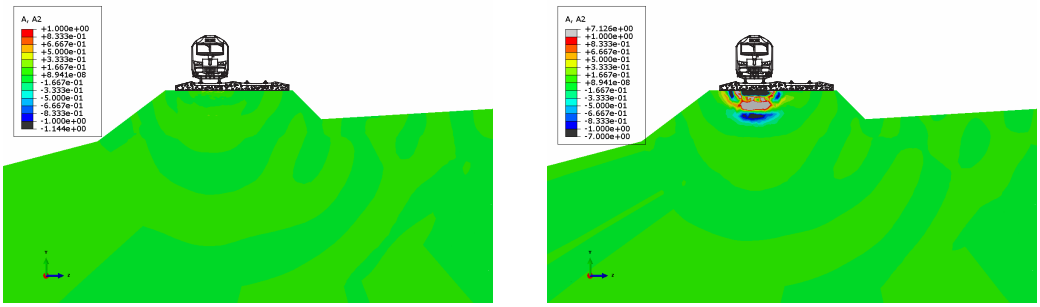

(a) (b)

Figure 8: Numerical visualisation (x-axis planar view) of the passage of an AM96 trainset at a speed of $120\,\mathrm{km/h}$ (a) without defect and (b) with a $40\,\mathrm{mm}$ length negative pulse defect.

4.4 Influence of the vehicle speed

The previous section is devoted to the variation in vehicle speed levels ($v_0 = 100\,\mathrm{km/h}$, $120\,\mathrm{km/h}$ and $140\,\mathrm{km/h}$). Figure 9 presents, for some studied defect, the variation in PPV. Note that the two defects — step-down stepwise joint and wheel flat — present the same characteristics, confirming that these defects are not greatly effected by train speed (in this case, the effect with the speed is associated with the quasi-static contribution of the vehicle only). Despite this, for some defects (e. g. smooth irregularity), the higher the vehicle speed, the greater the ground vibration level. For other defects (e.g. step-down joint), the opposite is true. To understand this difference, a frequency content study of the ground vibration signal is necessary.

Therefore Figure 10 shows the corresponding frequency content in the case of the step-up joint. For each speed, an additional curve representing the amplitude modulation, due to the fundamental axle passage frequency, is added. This illustrates that the frequency content of the initial defect impact content is also modulated by the axle periodicity [19]. The maximum amplitude of vibration generated by the defect impact can be inside the lobes (Figures 10(a) and 10(c)) or between two lobes (Figure 10(b)).

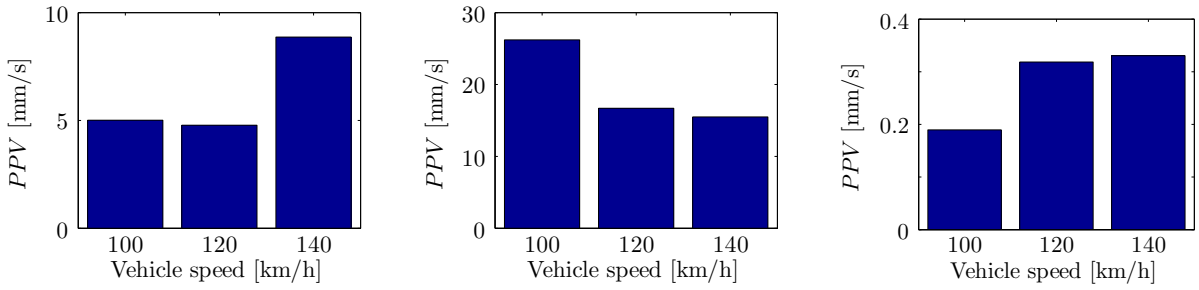

Figure 9: Peak particle velocity as a function of the vehicle speed at $10\,\mathrm{m}$ from the track and for an AM96 trainset running on (a) smooth irregularity ($l = 200\,\mathrm{mm}$, $h = 5\,\mathrm{mm}$), (b) step-down joint ($h = 5\,\mathrm{mm}$) and (c) wheel flat ($r = 50\,\mathrm{mm}$).

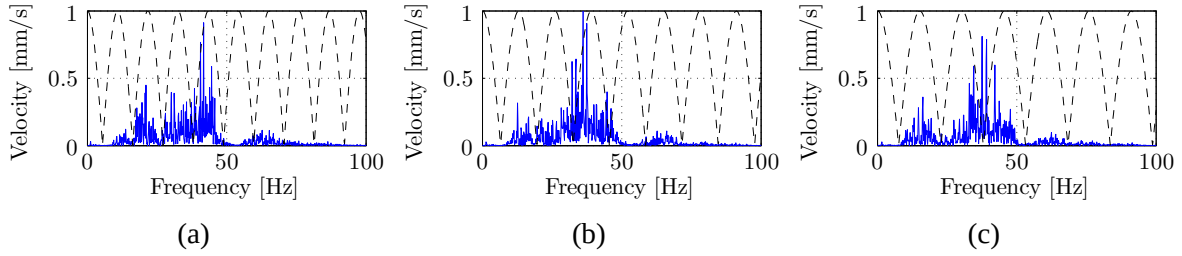

Figure 10: Frequency content of ground vibrations calculated at $10\,\mathrm{m}$ from the track for the step-up joint ($h = 5\,\mathrm{mm}$) and for a speed of (a) $v_0 = 100\,\mathrm{km/h}$, (b) $v_0 = 120\,\mathrm{km/h}$ and (c) $v_0 = 140\,\mathrm{km/h}$ (the dash lines represent the amplitude modulation due to the fundamental axle passage frequency).

5 CONCLUSION

Ground-borne vibration from railway traffic is becoming an increasing problem, particularly in urban environments. A common source of this vibration is individual, localised local defects which generate large amplitude excitations.

This study uses a time domain vibration prediction model is used to investigate the vibrations generated at the wheel/rail contact due to these defects. Different types of rail and wheel defect are mathematically modelled, including rail joints, switches, crossings and wheel flats. The problem was broken into two sub-models: one for the train-track and one for the soil. This work focuses on the AM96 trainset, largely used in the Brussels Region (Belgium). The geometries of a variety of local defect types are analysed and a sensitivity analysis is undertaken based upon the defect size and train speed. It is found that defect type and geometry have a significant influence on vibration levels, and that only selected geometry types are effected by train speed.

ACKNOWLEDGEMENT

The first author would like to acknowledge, Sébastien Mercier and Joseph Tsongo, from the Faculty of Engineering of the University of Mons, for their investigations into the local defect analysis.

REFERENCES

[1] C. Madshus and A. M. Kaynia. High-speed railway lines on soft ground: dynamic behaviour at critical train speed. *Journal of Sound and Vibration*, 231(3):689–701, 2000.

[2] D. P. Connolly, G. Kouroussis, O. Laghrouche, C. Ho, and M. C. Forde. Benchmarking railway vibrations — track, vehicle, ground and building effects. *Construction and Building Materials*, doi: 10.1016/j.conbuildmat.2014.07.042 (in press), 2014.

[3] D. P. Connolly, G. Kouroussis, P. K. Woodward, P. A. Costa, O. Verlinden, and M. C. Forde. Field testing and analysis of high speed rail vibrations. *Soil Dynamics and Earthquake Engineering*, 67:102–118, 2014.

[4] L. Auersch and S. Said. Attenuation of ground vibrations due to different technical sources. *Earthquake Engineering and Engineering Vibration*, 9:337–344, 2010.

[5] D. P. Connolly, G. Kouroussis, P. K. Woodward, O. Verlinden, A. Giannopoulos, and M. C. Forde. Scoping prediction of re-radiated ground-borne noise and vibration near high speed rail lines with variable soils. *Soil Dynamics and Earthquake Engineering*, 66:78–88, 2014.

[6] J. C. O. Nielsen and T. J. S. Abrahamsson. Coupling of physical and modal components for analysis of moving non-linear dynamic systems on general beam structures. *International Journal for Numerical Methods in Engineering*, 33(9):1843–1859, 1992.

[7] W. Zhai and X. Sun. A detailed model for investigating vertical interaction between railway vehicle and track. *Vehicle System Dynamics*, 23(supplement):603–615, 1994.

[8] J. Oscarsson and T. Dahlberg. Dynamic train/track/ballast interaction - computer models and full-scale experiments. *Vehicle System Dynamics*, 29(supplement):73–84, 1998.

[9] C. Andersson and J. Oscarsson. Dynamic train/track interaction including state-dependent track properties and flexible vehicle components. *Vehicle System Dynamics*, 33(supplement):47–58, 1999.

[10] G. Kouroussis, G. Gazetas, I. Anastasopoulos, C. Conti, and O. Verlinden. Discrete modelling of vertical track–soil coupling for vehicle–track dynamics. *Soil Dynamics and Earthquake Engineering*, 31(12):1711–1723, 2011.

[11] G. Kouroussis and O. Verlinden. Prediction of railway ground vibrations: accuracy of a coupled lumped mass model for representing the track/soil interaction. *Soil Dynamics and Earthquake Engineering*, 69:220–226, 2015.

[12] D. Younesian, S. R. Marjani, and E. Esmailzadeh. Importance of flexural mode shapes in dynamic analysis of high-speed trains traveling on bridges. *Journal of Vibration and Control*, 20(10):1565–1583, 2014.

[13] X. Zhao, Z. Li, and J. Liu. Wheel–rail impact and the dynamic forces at discrete supports of rails in the presence of singular rail surface defects. *Journal of Rail and Rapid Transit*, 226(2):124–139, 2012.

[14] G. Kouroussis, O. Verlinden, and C. Conti. Efficiency of resilient wheels on the alleviation of railway ground vibrations. *Journal of Rail and Rapid Transit*, 226(4):381–396, 2012.

[15] G. Alexandrou, G. Kouroussis, and O. Verlinden. A comprehensive prediction model for vehicle/track/soil dynamic response due to wheel flats. *Journal of Rail and Rapid Transit*, doi: 10.1177/0954409715576015 (in press), 2015.

[16] K. Vogiatzis. Noise and vibration theoretical evaluation and monitoring program for the protection of the Ancient "Kapnikarea Church" from Athens metro operation. *International Review of Civil Engineering*, 1:328–333, 2010.

[17] K. Vogiatzis. Protection of the cultural heritage from underground metro vibration and ground-borne noise in Athens centre: The case of the Kerameikos archaeological museum and Gazi cultural centre. *International Journal of Acoustics and Vibration*, 17:59–72, 2012.

[18] P. A. Costa, R. Calçada, and A. S. Cardoso. Influence of train dynamic modelling strategy on the prediction of track–ground vibrations induced by railway traffic. *Journal of Rail and Rapid Transit*, 226(4):434–450, 2012.

[19] G. Kouroussis, D. P. Connolly, and O. Verlinden. Railway induced ground vibrations — a review of vehicle effects. *International Journal of Rail Transportation*, 2(2):69–110, 2014.

[20] G. Kouroussis, C. Conti, and O. Verlinden. Experimental study of ground vibrations induced by Brussels IC/IR trains in their neighbourhood. *Mechanics & Industry*, 14(02):99–105, 2013.

[21] G. Kouroussis, J. Florentin, and O. Verlinden. Ground vibrations induced by intercity/interregion trains: A numerical prediction based on the multibody/finite element modeling approach. *Journal of Vibration and Control*, doi: 10.1177/1077546315573914 (in press), 2015.

[22] G. Kouroussis, L. Van Parys, C. Conti, and O. Verlinden. Prediction of ground vibrations induced by urban railway traffic: an analysis of the coupling assumptions between vehicle, track, soil, and buildings. *International Journal of Acoustics and Vibration*, 18(4):163–172, 2013.

[23] O. Verlinden, L. Ben Fekih, and G. Kouroussis. Symbolic generation of the kinematics of multibody systems in EasyDyn: from MuPAD to Xcas/Giac. *Theoretical & Applied Mechanics Letters*, 3(1):013012, 2013.

[24] G. Kouroussis, L. Van Parys, C. Conti, and O. Verlinden. Using three-dimensional finite element analysis in time domain to model railway–induced ground vibrations. *Advances in Engineering Software*, 70:63–76, 2014.